ChemComm

Accepted Manuscript

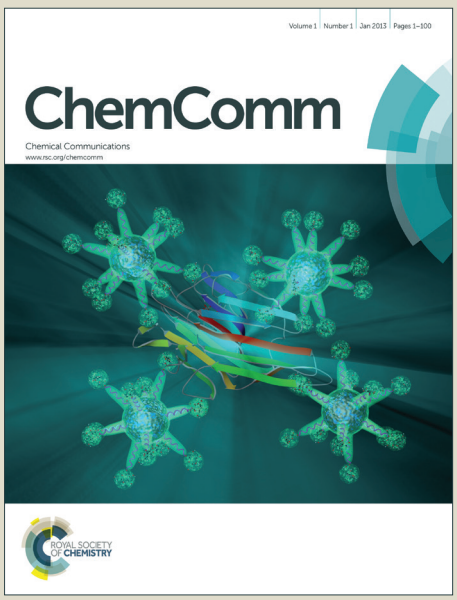

ROYAL SOCIETY OF CHEMISTRY

www.rsc.org/chemcomm

ChemComm

RSCPublishing

COMMUNICATION

Photodynamic optical sensor for buffer capacity and pH based on hydrogel-incorporated spiropyran

Cite this: DOI: 10.1039/xoxxoooooox

G. Mistlberger,[*a] M. Pawlak‡[b], E. Bakker[b] and I. Klimant[a]

Received ooth January 2012,
Accepted ooth January 2012

DOI: 10.1039/xoxxoooooox

www.rsc.org/

We introduce here a dynamic optode for buffer capacity sensing based on photochromic spiropyran (Sp). It represents the first reversible optical sensor for buffer capacity. Sensing was possible using a non-equilibrium readout mode, a novelty for photoswitchable optical ion sensors. In addition to the buffer capacity, the final point of each measurement sequence provides the pH of the solution.

Optical sensors for the measurement of pH and other ionic species are well understood and found many applications in science and industry.[1] Apart from solution based indicators for both protons and ions, interest in immobilized indicators increased during the last decades. Immobilization has many advantages, such as reduced toxicity, exclusion of interfering species, reduced cross-sensitivity to ionic strength and increased signal due to higher dye concentrations.[2] Indicator dyes for protons where mainly embedded into hydrogels for the production of optical pH sensors. Ionophore based bulk optodes, on the other hand, usually rely on the ion exchange or coextraction of protons with the target cation or anion.[3] Both of these systems were usually employed in a purely passive mode that is the sensors were immersed in the sample and the reading collected after equilibration with the sample provided information about the analyte concentration.

Transforming such passive systems into active optical ion sensors is possible by replacing the active compounds, such as pH indicator, ionophore or ion exchanger with photoswitchable analogues which, upon irradiation with light, change their affinity to their target.[3a] In the first attempts for producing photoresponsive materials that allow a triggered exchange of protons with specific cations, researchers utilized irreversible photoacid generators together with ionophores inside hydrophobic matrix materials.[4]

The next obvious step was to replace the irreversible photoacid generators with photoactive compounds which change their affinity towards protons upon illumination in a fully reversible way. An especially promising candidate for such compounds is the well-known photochromic dye spiropyran (Sp).[5] Illumination of Sp with UV light exposes a previously masked phenolic group and thereby changes its pK_a values by more than 6 units (Scheme 1).[6] Moreover, the activated form acts as pH indicator in both absorbance and fluorescence mode. Finally, the back reaction to the optically silent, closed form can be accelerated using light of a different wavelength, preferably >410 nm.

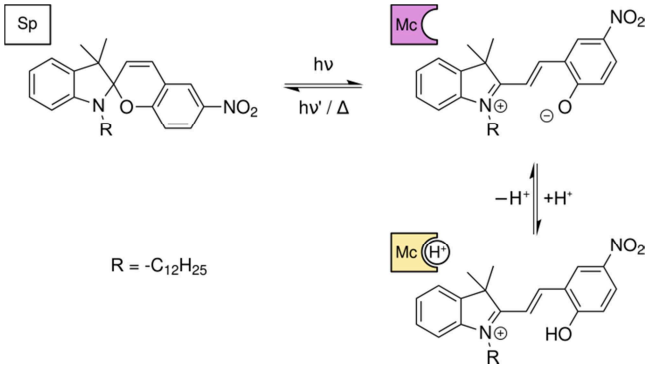

Scheme 1. Spiropyran (Sp) is converted to the ring opened merocyanine form (Mc) which acts as pH indicator changing its color form purple to yellow upon protonation.

Taking advantage of these properties, researchers developed optical sensors for chloride,[7] calcium and sodium[8] which can be switched on and off, where the off mode means that ion-exchange or coextraction is suppressed due to the low pK_a values of the closed form. Xie et al. also developed nanospheres for reversible extraction and release of potassium.[9] Although all these applications make use of spiropyran as a photoactive compound, the basic readout step is still equilibrium based.

In this work, we take full advantage of the suggested potential of Sp as photodynamic compound and present for the first time a truly kinetic readout scheme. As a model parameter we chose buffer capacity due to its importance in environmental questions as well as in biological research and in industry.[10] Although titration-based

buffer capacity measurements are routinely performed using autotitrators, this procedure is significantly more complex in submersible systems for environmental or bioprocess monitoring which would require a fluidic set-up with reagent containers. Only very few concepts were presented so far for 'hands-free' buffer capacity sensors which do not require addition of reagents. One of these concepts was based on the electrochemical production of acid and base close to an ISFET pH sensor.[11] In a similar approach, Bakker and co-workers developed a system for direct alkalinity measurements based on a flash chronopotentiometry titration.[12] An optical detection system based on irreversible photoacid generation was introduced earlier by Shvarev and evaluated for buffer capacity measurements.[4a] However, the irreversible nature of such systems limits the use in real-world applications.

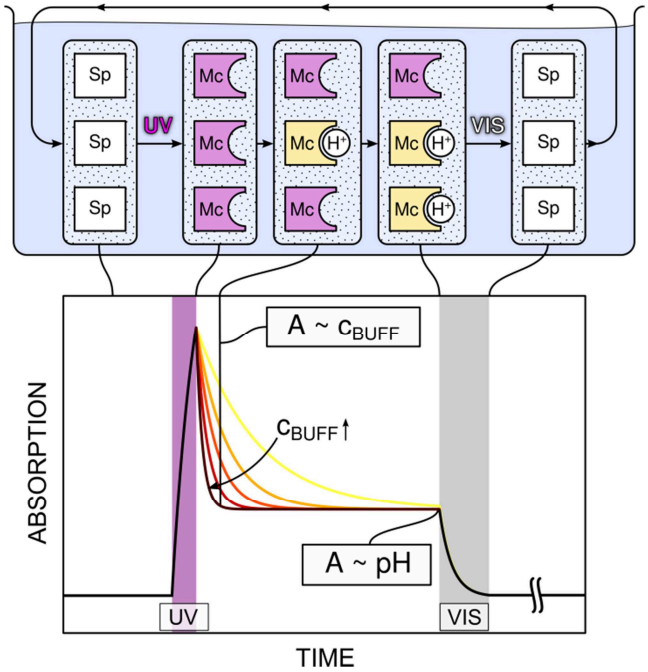

Fig. 1. Schematic representation of the processes involved in a typical buffer capacity measurement cycle using the current methodology. After 1 second illumination with a UV LED, protonation of the colored Mc-form starts. After a certain time interval the absorption signal depends only on the buffer capacity at a given pH value. After full equilibration with the sample solution, the absorption is a function of the pH value. Visible light is then used to regenerate the original state of the sensor and after equilibration with the sample a new cycle can start.

Here we present a novel kind of a titration-free buffer capacity optode. The basic processes involved in a measurement cycle are outlined in Fig. 1. A polyurethane hydrogel film containing Sp is immersed in the sample solution. After illumination with a UV pulse the Sp transforms into the colored, deprotonated Mc form. Protonation of Mc follows a buffer capacity-dependent kinetic. In a certain time range after the activation pulse, the absorption is a function of the buffer capacity (A ~ c_{Buff}), while full equilibration with the sample solution results in a pH-dependent absorbance value (A ~ pH). A subsequent pulse from a white LED regenerates the original state of the sensor. Protons are released from Mc and equilibrate with the sample solution. A new cycle can begin.

The sensor film consisted of Sp (6.2 mg, 77 mmol kg^{-1}, in-lab synthesis based on Datillo et al.[13]), the lipophilic salt Na-tetrakis[3,5-bis(trifluoromethyl)phenyl]borate (38.1 mg, 256 mmol kg^{-1}, www.sigmaaldrich.com) and hydrogel Hydromed D7 (168 mg, www.advbiomaterials.com). The lipophilic salt was required to increase the apparent pK_a values of the dye from ~3.4 to 5.7 due to stabilization of the protonated McH^+ form inside the hydrogel. The sensor components were dissolved in chloroform (496 mg) and knife-coated onto 125 µm poly(ethylene terephthalate) supports at thicknesses of 3 µm for the pH calibration and 9 µm for the buffer capacity measurements. The foils were then mounted into a custom made flow cell inside a UV/Vis spectrometer (Cary 60, www.agilent.com). High-power UV (APG2C1-375-E, www.roithner-laser.com) and white LEDs (SR-03-WN300, www.luxeonstar.com) were also mounted inside the spectrometer in order to allow for a reproducible switching of Sp to Mc and vice versa without disturbing the set-up (Fig. 2).

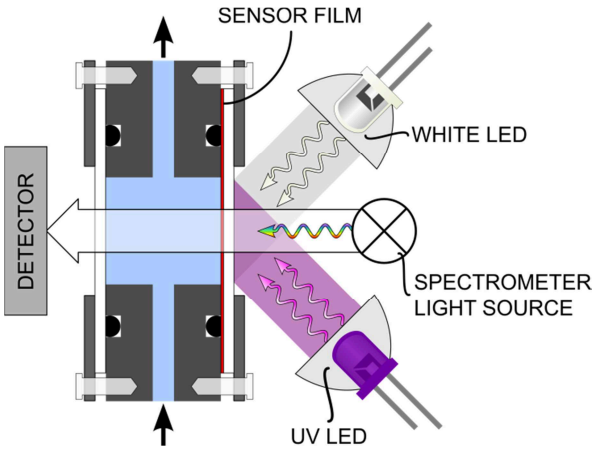

Fig. 2. Schematic representation of the flow cell used for this proof-of-concept study. The cell and the high-power UV- and white LEDs were mounted inside a UV/Vis spectrometer.

For the pH calibration the sensor foil was illuminated with a 4 s UV pulse. Afterwards, the flow cell was flushed with universal buffer solution at 28 mL min^{-1} while externally adjusting the pH using 2 M NaOH or HCl. The calibration shown in Fig. 3b reveals an apparent pK_a value of 5.7, which is slightly too low for measurements under physiological conditions. The protonation degree 1-α^* was calculated using a ratiometric approach according to Mistlberger et al. using the equation

$$1-\alpha^* = \left(1+\frac{A_{420,\max}}{A_{420,\min}}\cdot\frac{R-R_{\min}}{R_{\max}-R}\right)^{-1}$$

where $R = A_{560}/A_{420}$, $R_{min} = A_{560,min}/A_{420,max}$ and $R_{max}=A_{560,max}/A_{420,min}$.[3a] The ratiometric evaluation eliminates drift due to thermal deactivation during the calibration.

The slightly distorted isosbestic point in the spectra in Fig. 3a is due to thermal Mc→Sp reaction during the calibration and may also be enhanced by a potential migration of the dye inside the hydrogel during protonation. We observed this phenomenon with other dyes in the same matrix with negligible effect on the resulting calibrations.

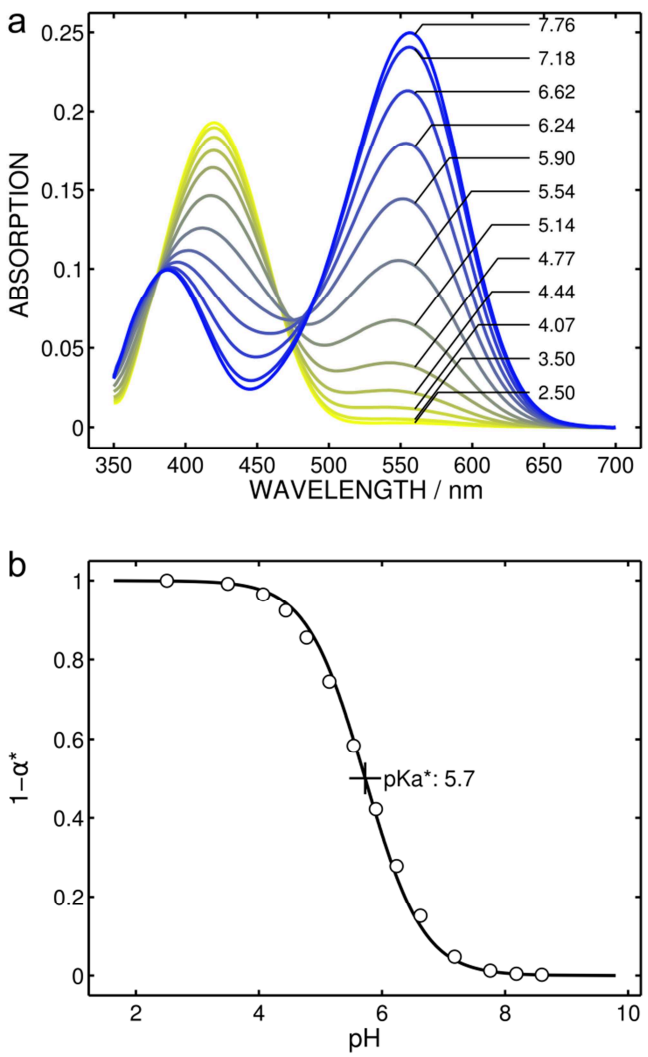

Fig. 3. pH calibration of the sensor film. (a) Absorption spectra collected at various pH values as indicated. (b) Calibration curve showing an apparent pK_a^* value of 5.7 at 1-α^* = 0.5.

For investigating the response of the sensor to various buffer concentrations, a thicker film was used to make sure that the main kinetic response originates from proton diffusion inside the hydrogel. After a 1 second UV pulse, the absorption was recorded at 560 nm, which is the maximum of the deprotonated species Mc. We investigated the response in acetate-MES buffers of three different pH values (4.6, 5.6 and 6.6) and concentrations of 2, 5, 10, 15, 20, 30 and 100 mM in a background of 0.5 M NaCl.

The measurements were carried out once under stopped flow conditions and once while flushing the flow cell with the respective buffer at a flow rate of 28 mL min^{-1}. The resulting response curves can be seen in Fig. 4 a-c as decrease in absorption relative to the starting point. The good agreement of the two cycles with and without flow suggests that there is negligible analyte transport from the solution to the sensor film during the measurement, i.e. there is virtually no stirring effect during the first 5 seconds. The occasional deviations from the smooth response curves occurred in the measurements under flow conditions and originate from small air bubbles passing the light path (e.g. pH 4.6, 15 mM; pH 6.6, 2 mM).

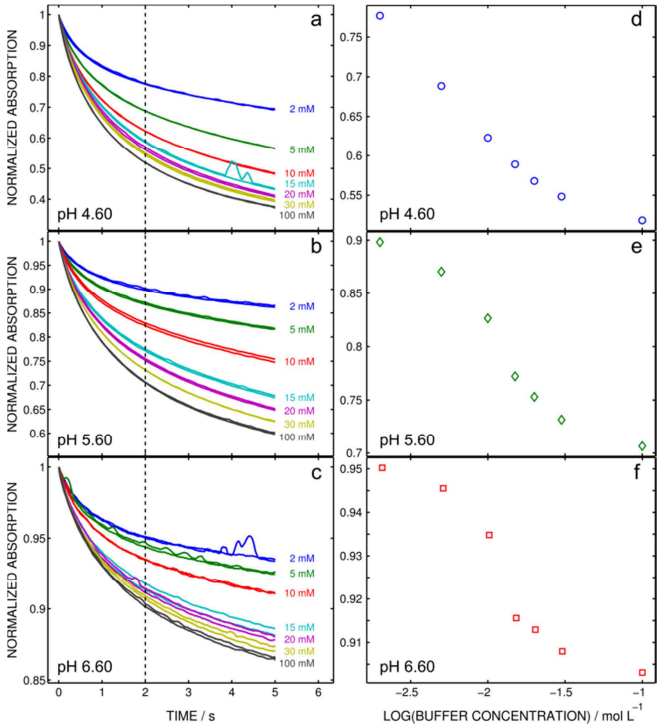

Fig. 4. Calibration of solutions with different buffer con-centrations. Three different pH values (4.6, 5.6 and 6.6) and 7 different buffer concentrations (2-100 mM) were investigated. (a-c) kinetic response at 560 nm (deprotonated form) during 5 seconds after the UV pulse. (d-e) absorption after 2 seconds vs. logarithmic buffer concentration.

Fig. 4 shows that the kinetic sensor response depends on both buffer concentration and pH value of the contacting sample solution. However, if one parameter is constant, the other one can be calibrated by plotting the relative absorbance change shortly after the activation pulse. In Fig. 4 d-e, the absorption 2 seconds after the UV pulse relative to the starting point was plotted against the logarithmic buffer concentration at constant pH. Obviously, at lower pH values the absolute signal change is larger which improves the signal-to-noise ratio. While a sample pH close to the pK_a^* value yields very reproducible results and a clear buffer capacity dependent dynamic response (Fig. 4 b and e), the noise and resolution of the calibration at pH 6.6 is significantly higher. Despite the decreased signal-to-noise ratio, the dynamic of the calibration curve still allows for a quantification of buffer capacity. This is important because currently limited options exist for dyes with similar photoswitching properties but with an increased pK_a value. This issue may be solved in the near future as photoswitching pH indicators with a higher pK_a value would also benefit the previously published, ion-selective sensor based on this system. Moreover, an intrinsically higher pK_a value could render the addition of lipophilic salt unnecessary, which would greatly reduce the cross-sensitivity to ionic strength.[14]

As mentioned in the explanation of Fig. 1, the final point of the kinetic response curves after full equilibration is theoretically independent of the buffer capacity but depends only on the pH of the buffer solution. Hence, the buffer capacity sensor can be simultaneously used as a pH sensor. Due to the increased film thickness in order to facilitate the kinetic evaluation of the absorbance changes, the response time of the pH sensor is too long for a convenient pH measurement. A full equilibration with the sample solution can take up to 10 minutes. In Fig. S1 in the supporting information, the kinetic response curves at pH 4.6 show

that even after 280 seconds, the film is not yet fully equilibrated with the sample solution. Moreover, a slight stirring effect was observed at 2 mM buffer concentration in the range 20-150 seconds, which indicates that there is a diffusion limitation on the sample side. Making a real dual-parameter sensor (pH and buffer capacity) requires further optimization of the film thickness, roughness and composition. These aspects are the topic of further studies on this novel type of sensor in our lab.

When working with Sp as photoactive compound, photostability is often an issue. Strategies for reducing the photobleaching during activation/deactivation of the dye included the covalent immobilization of the dye in order to avoid intermolecular deactivation of two Sp molecules in the excited state.[15] Although this strategy may also be beneficial for the current study, the results in Fig. 5 show that the photostability is more than sufficient at the proof-of-concept stage. For testing the reversibility, we immersed the sensor film in a solution of pH 8.9 and applied 200 cycles of the illumination sequence used for the measurements of buffer capacity, i.e. 1 sec UV and 5 sec white light. Although there is still some bleaching visible in the ON state, a loss of 0.1% per cycle is an acceptable decay and even outperforms the system of Radu et al. with immobilized spiropyran, where a decrease in absorbance of 2% per cycle was observed. This can be explained by the vastly reduced illumination time required for one measurement (1 sec UV, 5 sec white light vs. 60 sec UV, 60 sec white light).

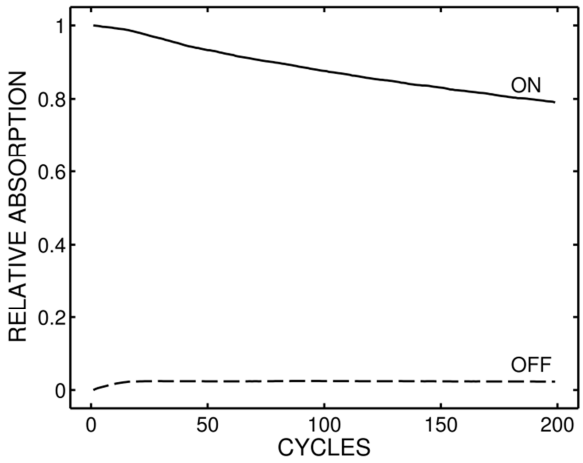

Fig. 5. Reversibility of the photoswitching process. The sensor film was immersed in buffer with a pH of 8.9 and exposed to 200 cycles of the following illumination: 1 s UV, 2 s dark, 5 s white, 2 s dark.

To conclude, we presented for the first time a reversible optode for buffer capacity. The sensor has the potential to vastly reduce the workload required for buffer capacity measurements by making titrations obsolete. It takes advantage of the unique properties of photoswitchable pH indicators, which allow an in situ activation and regeneration of the sensor using light of different wavelengths, a task impossible using conventional, passive sensors. This is also the first time that a sensor of this type was evaluated in dynamic mode. Finally, in principle the sensor can be used for measuring both buffer capacity and pH with one and the same sensor.

G. Mistlberger gratefully acknowledges the support by the Austrian Science Fund (FWF): J3343.

Notes and references

[a] Graz University of Technology, Institute of Analytical Chemistry and Food Chemistry, 8010 Graz, Austria. E-mail: g.mistlberger@gmail.com

[b] University of Geneva, Department of Inorganic and Analytical Chemistry, 1211 Geneva 4, Switzerland.

‡ Current address: Optiqua Technologies, 82 WaterHub Toh Guan Road East #C2-11/1, 608576 Singapore

†Electronic Supplementary Information (ESI) available: Figure showing the kinetic response at pH 4.6 over a prolonged period. See DOI: 10.1039/c000000x/

1 a) D. Wencel, T. Abel, C. McDonagh, *Anal. Chem.* **2014**, 86, 15–29; b) C. McDonagh, C. S. Burke, B. D. MacCraith, *Chem. Rev.* **2008**, 108, 400–422; c) X.-D. Wang, O. S. Wolfbeis, *Anal. Chem.* **2013**, 85, 487–508; d) O. S. Wolfbeis, *Adv. Mater.* **2008**, 20, 3759–3763.

2 a) J. Lin, TrAC Trends *Anal. Chem.* **2000**, 19, 541–552; b) C. R. Schröder, B. M. Weidgans, I. Klimant, *Analyst* **2005**, 130, 907.

3 a) G. Mistlberger, G. A. Crespo, E. Bakker, *Annu. Rev. Anal. Chem.* **2014**, 7, 483–512; E. Bakker, P. Bühlmann, E. Pretsch, *Chem. Rev.* **1997**, 97, 3083–3132.

4 a) A. Shvarev, *J. Am. Chem. Soc.* **2006**, 128, 7138–7139; b) X. Xie, G. Mistlberger, E. Bakker, *Sens. Actuators B Chem.* **2014**, DOI 10.1016/j.snb.2014.08.041.

5 V. I. Minkin, *Chem. Rev.* **2004**, 104, 2751–2776.

6 G. Mistlberger, G. A. Crespo, X. Xie, E. Bakker, *Chem. Commun.* **2012**, 48, 5662–5664.

7 X. Xie, G. Mistlberger, E. Bakker, *J. Am. Chem. Soc.* **2012**, 134, 16929–16932.

8 G. Mistlberger, X. Xie, M. Pawlak, G. A. Crespo, E. Bakker, *Anal. Chem.* **2013**, 85, 2983–2990.

9 X. Xie, E. Bakker, *ACS Appl. Mater. Interfaces* **2014**, 6, 2666–2670.

10 a) H. Elderfield, *Science* 2002, 296, 1618–1621; b) B. O'Rourke, L. A. Blatter, *J. Mol. Cell. Cardiol.* **2009**, 46, 767–774; c) A. G. Asuero, T. Michałowski, *Crit. Rev. Anal. Chem.* **2011**, 41, 151–187.

11 J. Luo, W. Olthuis, P. Bergveld, M. Bos, W. E. van der Linden, *Sens. Actuators B Chem.* **1994**, 20, 7–15.

12 a) M. G. Afshar, G. A. Crespo, X. Xie, E. Bakker, *Anal. Chem.* **2014**, 86, 6461–6470; b) G. A. Crespo, M. Ghahraman Afshar, E. Bakker, *Anal. Chem.* **2012**, 84, 10165–10169.

13 D. Dattilo, L. Armelao, G. Fois, G. Mistura, M. Maggini, *Langmuir* **2007**, 23, 12945–12950.

14 B. M. Weidgans, C. Krause, I. Klimant, O. S. Wolfbeis, *Analyst* **2004**, 129, 645–650.

15 A. Radu, R. Byrne, N. Alhashimy, M. Fusaro, S. Scarmagnani, D. Diamond, *J. Photochem. Photobiol. Chem.* **2009**, 206, 109–115.

ChemComm RSCPublishing

Graphical Abstract

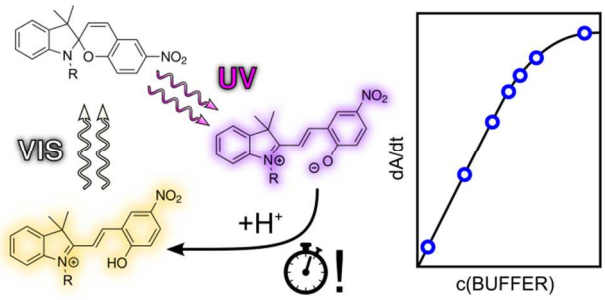

The kinetics of a light activated proton extraction correlates with the buffer capacity of a sample at a given pH.